JOURNAL OF MATERIALS SCIENCE 18 (1983) 3404–3408

Hygrothermal ageing and fracture of glass fibre–epoxy composites

PAUL D. ANSTICE
Hunting Engineering Ltd., Reddings Wood, Ampthill, Bedfordshire, UK
PETER W. R. BEAUMONT
Engineering Department, Cambridge University, Trumpington Street, Cambridge, UK

The effects of hygrothermal ageing upon the failure characteristics and work of fracture of glass fibres in epoxy are described. A collection of data based on the direct observation and measurement of fibre debond length and fibre pull-out length after fracture is displayed in empirical failure diagrams. Similarly, a vast number of experimental measurements of work of fracture is displayed in a three-dimensional diagram where the axes are work of fracture, humidity and ageing time. This information is combined with models of fracture in the construction of a fracture map which is used to interpret hygrothermal ageing phenomena.

1. Introduction

1.1. Fracture mechanisms

Fibrous composites fail by a number of mechanisms: fibre fracture, matrix cracking fibre–matrix decohesion (debonding or interfacial cracking), fibre pull-out and so forth. Each fracture process has certain characteristics; the stress and location at which a fibre breaks, for example, depends upon the size and distribution of flaws along the fibre length; interfacial failure is sensitive to the nature of the fibre–matrix bond and fibre–matrix misfit strain*. The magnitude and distribution of fibre strength affect two characteristic failure parameters which we call fibre debond length, l_d, and fibre pull-out length, l_p, i.e. distances over which an intact fibre debonds and finally pulls out of a cracked matrix under monotonic loading. These failure processes are likely to be influenced by temperature and humidity in the air and be time-dependent in an hygrothermal ageing experiment. An understanding of them is important because they determine the work of fracture or toughness of the composite.

We have assembled a large collection of fractographic data based on the two failure parameters l_d and l_p for aligned glass fibres in epoxy. The data are displayed in diagrams which show the distribution of fibre debond lengths and fibre pull-out lengths in a given experiment. The effects of changing humidity or time of exposure can be seen. We also present a large amount of data on work of fracture in a three-dimensional diagram where the axes are work of fracture, humidity and hygrothermal ageing time. The effects of humidity and time of exposure upon the toughness of the composite are clear.

1.2. Toughness relationships

Each mechanism of fracture can be modelled and the associated dissipation of energy described by a set of equations of the generalized form

$$G = f(\sigma_f, E_f, \sigma_m, E_m, \mu, \nu_f, \nu_m, G_m, G_i, \epsilon_0, \text{etc.})$$

These are some of the material variables which describe the properties of the composite and its microstructural features: fibre strength, σ_f, and stiffness, E_f, polymer strength, σ_m, and stiffness, E_m, coefficient of friction at the interface, μ, Poisson ratio of fibre, ν_f, and polymer, ν_m, matrix and interfacial toughness, G_m and G_i, and fibre–matrix misfit strain ϵ_0. Some of these parameters are likely to be affected by adsorbed moisture,

*The fibre–matrix misfit strain is related to the localized radial stresses around fibres, its magnitude is sensitive to the amount of shrinkage of the matrix during curing and cooling from the fabrication temperature [1].

0022–2461/83 $03.00 + .12

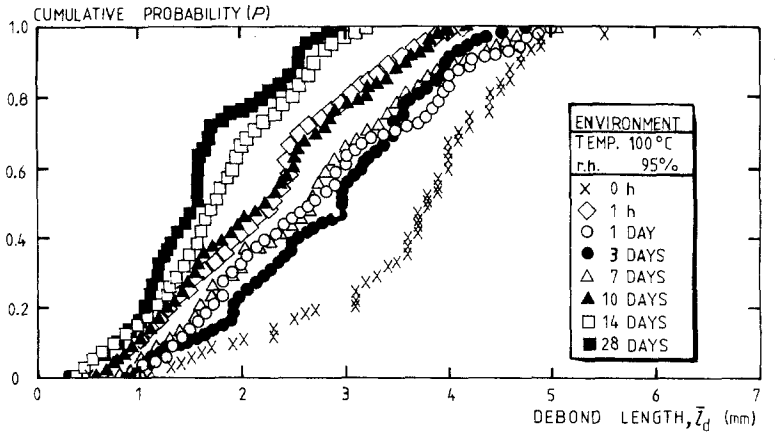

Figure 1 The distribution of debond length data for a model, unidirectional glass fibre–epoxy composite. Hygrothermal ageing occurred in air at 100° C, 95% r.h.

σ_f, E_m, ϵ_0, μ, for instance, and they may change with time in a hygrothermal ageing experiment.

Although we have satisfactory physical models that lead to a set of toughness equations (Wells [1] has reviewed these models and improved them), we do not understand how some of the terms which appear in these equations are affected by certain extrinsic conditions such as humidity and time of exposure to moisture. The development of these models to take into account environmental effects is incomplete and there exist little data on which to evaluate them.

We have collected and superimposed some work of fracture data of a (0°/90°) glass fibre–epoxy composite onto a fracture map which is based on models of fracture. The effect of ageing time upon certain material parameters like fibre strength and the fibre–matrix misfit strain and how they affect the work of fracture can be read directly from the map. The map also helps to interpret the origins of hygrothermal degradation.

2. Failure analysis and work of fracture

Figs. 1–4 show typical failure diagrams for a model unidirectional glass fibre–epoxy composite. (Details of these model composites, their design, manufacture and testing have been reported in previous issues of the Journal [2, 3].) The diagram shows, on axes of cumulative probability and fibre length, the effect of time in an hygrothermal ageing experiment upon the distribution of debond and pull-out length data. Such data was obtained in a failure analysis of specimens broken in tension at room temperature [3]. We see an initial displacement of debond length data to higher values between 1 and 72 h of exposure to 95% relative humidity (r.h.), 100° C, followed by a steady movement of data to lower values beyond 3 days (Fig. 1). For some reason, the data collected on unaged material ($t = 0$) appears in the diagram to be out of position*.

Measurements of glass fibre pull-out lengths are an order of magnitude less than the observed debond lengths (Fig. 2) and data fall into two distinct bands, longer pull-out lengths for 3 days exposure time or less, shorter pull-out lengths for longer ageing times. There seems to be an incu-

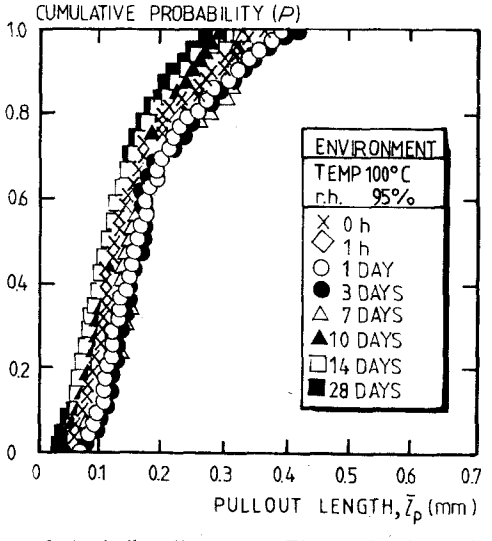

Figure 2 A similar diagram to Fig. 1, showing pull-out length data (100° C, 95% r.h.).

*We believe that residual localized compressive stresses are set-up in the matrix around a fibre when a sample is cooled from its fabrication temperature (100° C) to room temperature. In the case of unaged material, about 7 days elapsed between fabrication and testing, perhaps sufficient time for these residual stresses and the corresponding mismatch strain ϵ_0 between fibre and matrix to relax, the matrix compressive stress and interfacial shear stress for debonding to fall, and the fibre debond length to increase.

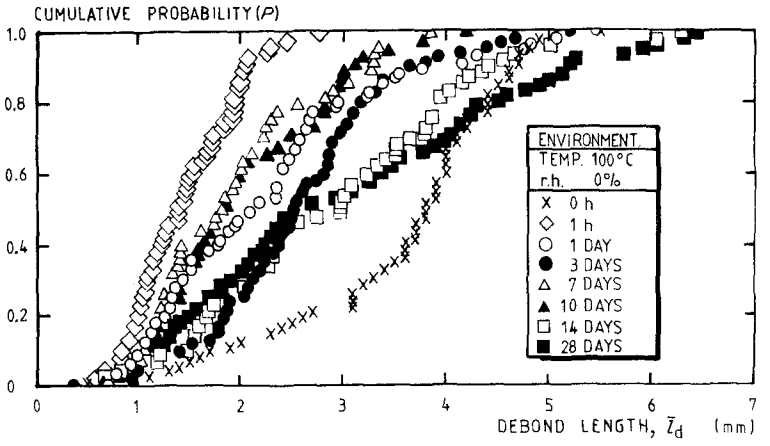

Figure 3 A similar diagram to Fig. 1, showing debond length data (100° C. 0% r.h.).

bation time of about 72 h before fibre debond and pull-out lengths begin to shorten. Figs. 3 and 4 show data for ageing at 100° C, 0% r.h. Each set of data does not superimpose but is displaced relative to one another. At short times, the debonded fibres lengthen and then fall; after 2 weeks, they increase in length once again. As we shall see in Fig. 5, these subtle movements of failure data curves reflect the observed changes in work of fracture with ageing.

The work of fracture can be summarized in a three-dimensional diagram with axes of work of fracture, humidity and ageing time (Fig. 5). The diagram is constructed by assembling a large collection of experimental data of work of fracture for different humidities and times of exposure.

In dry air (0% r.h.), a precipitous fall in work of fracture of the composite occurs during the first hour of exposure. Recovery is complete after about 1 day but the work of fracture slowly falls once again during the next 150 h or so. For even longer exposure times, we see a steady rise in work of fracture to exceed the original value. Exposure to higher humidities results in an early drop in work of fracture. This is followed by a recovery after 2 or 3 days, the work of fracture finally falling to about one-half of the original value after 4 weeks or more. Exposure to 95% r.h., 100° C causes the work of fracture to rise during the first 3 days or so, and then fall by more than one-half after a few weeks. Our explanation is that resin volume changes due to moisture uptake produces the initial increase in work of fracture, followed by fibre strength degradation and a loss of toughness [4] (see Section 3).

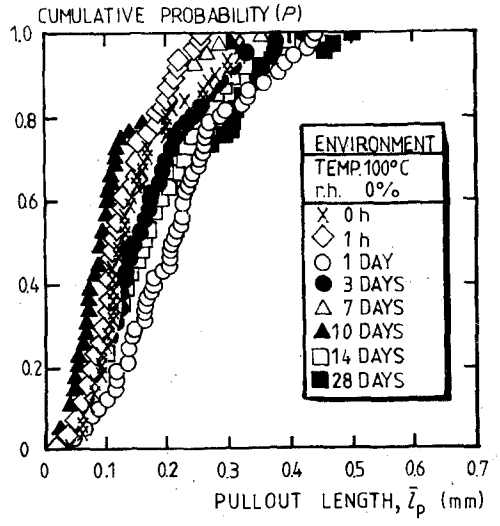

Figure 4 A similar diagram to Fig. 1, showing pull-out length data (100° C, 0% r.h.).

Our interpretation for the precipitous fall in fibre debond length and work of fracture after only 1 h of exposure to hot environments is to do with changes in magnitudes of the residual localized stresses around the fibre. We recall that "unaged" material was tested about 7 days after manufacture (see previous footnote). In that time, any residual stress in the matrix due to shrinkage during fabrication and cooling may have relaxed. The fibre load to initiate debonding decreases, and the fibre debond length and work of fracture both increase. (Models of fibre debonding show fibre debond length and work to fracture to be proportional to one another [1].)

The origin of the observed increase in work of fracture after 2 weeks and longer in hot, dry air may be due to a degradation of the fibre–matrix interface. Ishida and Koenig [5] have reported polymerization of silane coatings on glass fibres during prolonged exposure to high temperatures

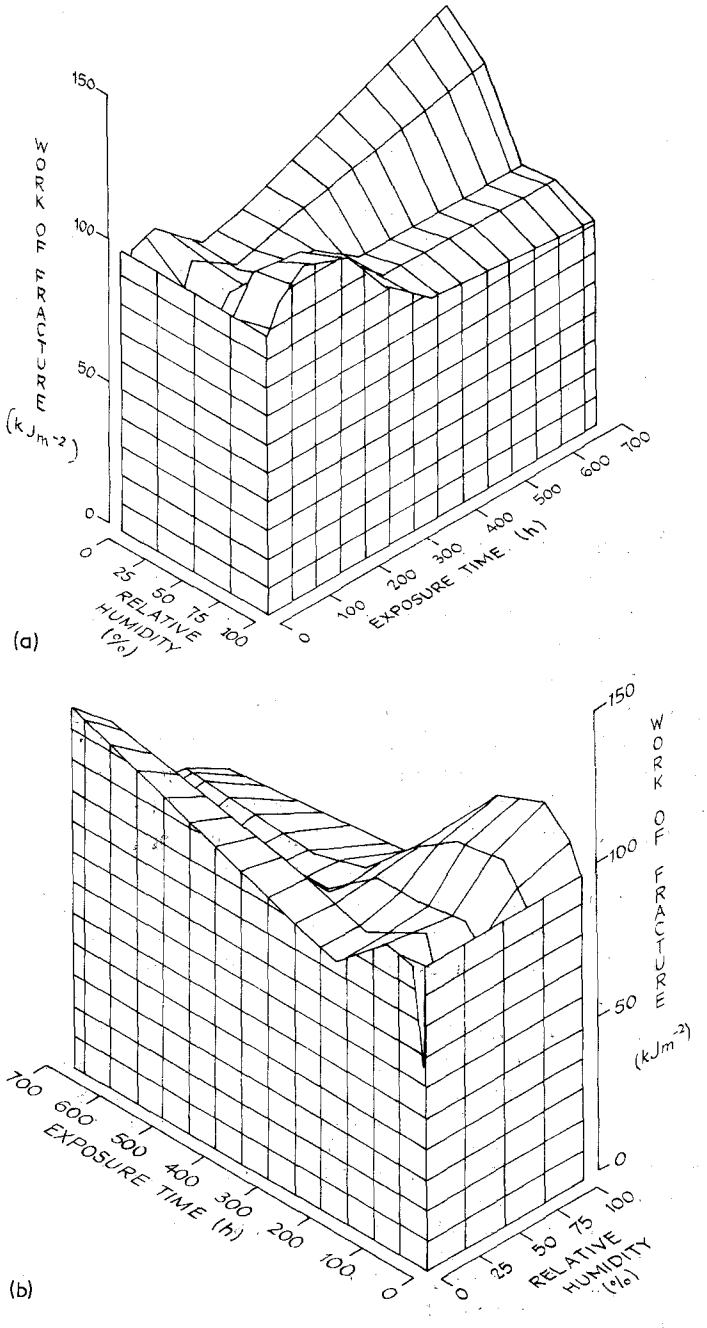

Figure 5 (a) and (b) diagrams with axes of work of fracture, humidity and ageing time. The large number of experimental work of fracture data have been removed from the diagram for the sake of clarity.

and a corresponding decrease in fibre–matrix bond strength.

3. Fracture maps

3.1. Construction and use of the map

First, the characteristic fibre debond length and fibre pull-out length are computed for given combinations of material properties, fibre strength, fibre stiffness, and so forth using models developed by Wells and Beaumont [6]. Combining these values with models of fracture [1] enables calculation of the theoretical work of fracture of the composite. The total predicted work of fracture is then normalized to twice the total cross-sectional area of the fibres. The map displays as contour lines information of predicted fibre debond lengths and fibre pull-out lengths, together with theoretical values of work of fracture. Comparison between theory and experiment enables the principal mechanism for fracture to be determined which is also shown on the map. We can then obtain some idea of the mechanisms of ageing.

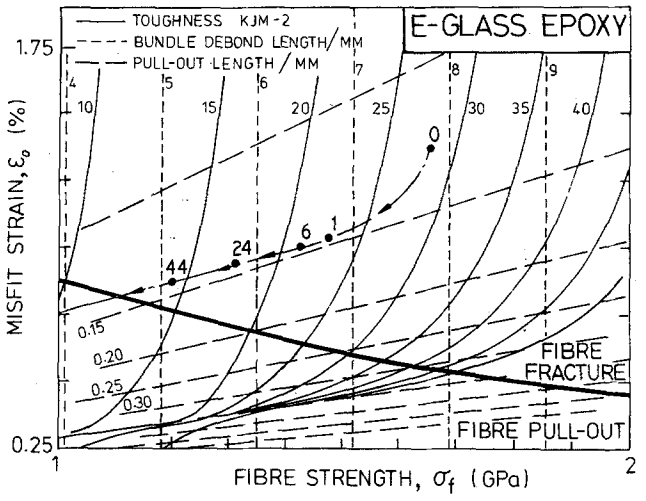

Figure 6 A typical fracture map for a (0°/90°) glass fibre–epoxy composite [6]. The contour lines represent variations of theoretical fibre debond length, pull-out length, and work of fracture with changes in fibre strength and fibre–matrix misfit strain. Some experimental work of fracture data is superimposed on the map and the arrows show the effect of increasing time. The number adjacent each datum point refers to the hours of exposure to air at 100° C, 95% r.h.

A typical fracture map for a (0°/90°) glass fibre–epoxy laminate is shown in Fig. 6. The axes are fibre–matrix misfit strain, ϵ_0 and fibre strength, σ_f. Superimposed onto the map are experimental data points of work of fracture. (The contour lines of fibre debond length together with measurements of debond length help to position the data.) The arrows show the direction in which movement of data occur with increasing ageing time at 100° C, 95% r.h., up to 100 h of exposure. We believe that the absorbed moisture causes the resin to swell and for the fibre–matrix misfit strain to fall. Also the fibre length decreases due to a stress-corrosion cracking mechanism between the glass and adsorbed water. The map shows these changes in σ_f and ϵ_0 consistent with observed trends in l_d and work of fracture.

4. Conclusions

Complicated phenomena involving competing mechanisms of fracture can be empirically analysed by displaying certain experimental failure data in appropriate diagrams. These diagrams show the distribution of important characteristic failure parameters, fibre debond length and fibre pull-out length, and the effects of hygrothermal ageing. Alternatively, fracture maps can be constructed which display information on these two failure parameters together with the work of fracture. These maps show the effect of moisture and time upon certain microscopic variables, fibre strength, fibre–matrix mismatch strain are examples, and the resultant influence on work of fracture.

Acknowledgements

We would like to thank the Science and Engineering Research Council for providing PDA with a post-doctoral research fellowship and for supporting current research at Cambridge. We also wish to thank Dr John K. Wells for computing the fracture map reported in this paper and for valuable discussions. The gift of fibres from Mr Leslie N. Phillips, formerly of the Royal Aircraft Establishment, Farnborough, is gratefully received.

References

1. J. K. WELLS, PhD thesis, University of Cambridge (1982).
2. J. N. KIRK, M. MUNRO and P. W. R. BEAUMONT, *J. Mater, Sci.* **13** (1978) 2197.
3. P. W. R. BEAUMONT and P. D. ANSTICE, *ibid.* **15** (1980) 2619.
4. J. K. WELLS and P. W. R. BEAUMONT, *ibid.* **17** (1982) 297.
5. H. ISHIDA and J. L. KOENIG, *J. Polym. Sci.* **17** (1979) 615.
6. J. K. WELLS and P. W. R. BEAUMONT, PRI meeting on Deformation, Yielding and Fracture of Polymers, Cambridge, March/April 1982.

Received 3 March
and accepted 17 March 1983